**International Journal of Science, Engineering & Environmental Technology (IJOSEET), 10(11): 50-62, 2023**

**ISSN 0749-9650**

www.repcomseet.org

# THE IMPACTS OF EXOTHERMIC CHEMICAL REACTION ON THE FORCED CONVECTION FLOW OF A THERMALLY RADIATIVE NON-NEWTONIAN BASED HYBRID NANOFLUID

**Ajala Augustine G.[1]*, Amola Benjamin A.[1], Akinrinmade Victor A.[2]**

[1] Department of Statistics, Federal Polytechnic Ede, Osun State, Nigeria,

[2]Osun State College of Technology, Esa Oke, Osun State, Nigeria.

* *Correspondence email address: ajalagbadebo744@gmail.com,*

**Abstract: This study considers the influence of exothermic – endothermic chemical reaction on the forced convection flow of a non-Newtonian fluid based hybrid nanofluid. In the cause of the study, thermal radiation and temperature dependent fluid parameters were put into consideration. Similarity transformation method was used to convert the governing equations of the problem to coupled ordinary differential equations and numerical solution thereafter was obtained. Effects of exothermic and endothermic reaction and radiation are then discussed based on the numerical solution.**

***Keywords:*** **Arrhenius activation energy, Casson fluid, endothermic reaction, exothermic reaction, Hybrid nanofluid, thermal radiation, radiation.**

## 1. Introduction

Heat transfer and fluid flow driven by an external source is an important concept in many of engineering applications. This is because the design and operation of evaporators, condensers, water-tube boilers and many other major items of chemical and power plants and water-cooled nuclear reactors is dependent on the knowledge of fluid dynamics and heat transfer process occurring during forced convective boiling [1]. In view of these, a sizeable number of experiments have been conducted in this direction. Trombetta [2] investigated the forced convection of a fully developed lamina flow in an eccentric annulus. The boundary layer flow together with heat transfer generated by the forced convection on a flat plate embedded in a porous medium was investigated by Beckermann and Viskanta [3]. Later, Childs and Long [4] analyzed the forced convective heat transfer in both stationary and rotational annuli. Forced convection near a forward stagnation point of an infinite plane wall powered by Newtonian heating was examined by Salleh *et al.* [5]. In company of chemical reaction, Moshizi [1] studied the forced convection heat and mass transfer of MHD nanofluid flow inside a porous channel.

The global demand for more energy was partly met by what is today known as nanofluid. By nanofluid, this refers to fluid with a nanoparticle of metal or oxide of metal infused in it. The idea is to increase the heat transfer ability of the fluid and develop substance of better efficiency. Nanofluid have wide use in electronics cooling, solar thermal systems, lubrication in mechanical systems, medical diagnostic imaging, catalytic converters, fuel cells, energy storage and so on. A new variant of nanofluid has been developed which is known as hybrid nanofluid. The hybrid nanofluid in its own case has more than one metallic nanoparticles in a base fluid. Findings have shown that the hybrid nanofluid displays a higher heat transfer rate and more efficiency than the conventional nanofluid. The first notable work on nanofluid can be accredited to Choi [6] when he discussed the use of nanoparticles in enhancing fluid thermal conductivity. The properties of Hybrid nanofluid and its heat transfer phenomenon was analyzed by Suresh *et al.*[7]. Thereafter, Nadeem *et al.* [8] deliberated on the importance of hybrid nanofluid over simple nanofluids. The impacts of magnetic dipole on hybrid nanofluid flow was studied by Gul *et al.*[9]. The flow of Cu-Al2O3 hybrid nanofluid over a moving permeable surface was examined by Aladdin *et al.*[10]. Taking a heated chamber as a case study, Rashidi *et al.* in [11] simulated the energy transference of a hybrid nanosuspension.

Chemical reaction is an important concept in numerous activities like combustion, filtration, absorption of substance in living organism, fermentation, food processes, polymer production and so on. Often times, chemical reaction is accompanied by energy. There is either a release of energy into the surrounding which is termed “exothermic” or absorption from the surrounding known as endothermic. The exothermic reaction finds place in production of energy for powering engines through the burning of coal, oil, gas; domestic heating and cooking; explosives in mining, construction and military operations. While endothermic on the other hand find solace in cooling sytems like refrigerating and air conditioning units, instant cold packs for first aid and sport injuries, photosynthesis and so on. These applications have enticed research to embark on some level of research on these phenomenon. Abdul Maleque Kh. [12] discussed the effects exothermic/endothermic chemical reactions on MHD free convection flow in presence of radiation.

Entropy generation minimization of higher order endothermic/exothermic chemical reaction on MHD mixed convection flow over stretching surface was investigated by Sharma *et al.*[13].

To the best of our knowledge, the influence of exothermic – endothermic chemical reaction on the forced convective flow of a third grade hybridnano fluid have not been investigated before hence the motivation to undertake this work. However, the main focus of this work is to establish the existence and uniqueness of solution to this problem.

## 2. Mathematical Formulation

A two-dimensional, steady, boundary layer flow of a hybrid nanofluid made up of Ag/Au nanoparticles is considered with a sodium alginate considered as the base fluid and the fluid flow past a half infinite plate moving in a uniformly free flow, $U$ as shown in Fig.1. Casson fluid model is used to express the properties of sodium alginate. The system is simulated in a way that the $x$-axis is aligned to the plate surface while the $y$-axis is the coordinate taken to be normal to the plate. The components of the hybrid nanofluid are assumed to be in thermal equilibrium with no slip condition. In addition, the ambient fluid velocity of the plate is considered to be $u_w = \delta U x$ where $\delta$ is the parameter for plate velocity [3]. The hybrid nanofluid’s thermophysical characteristics are engraved on Table 1.

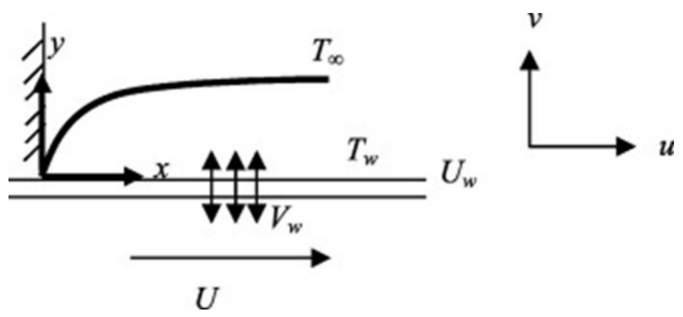


Fig 1: Flow configuration of the model

In view of the above presumptions along with ideas from past works [1,14,15], the governing equations for the model takes the form:

$$\frac{\partial u}{\partial x} + \frac{\partial v}{\partial y} = 0 \tag{1}$$

$$u\frac{\partial u}{\partial x} + v\frac{\partial u}{\partial y} = u_e\frac{du_e}{dx} + \frac{1}{\rho_{hnf}}\left(1+\frac{1}{\beta_c}\right)\frac{\partial}{\partial y}\left(\mu(T)\frac{\partial u}{\partial y}\right) - \frac{\sigma B^2(x)}{\rho_{hnf}}(u-u_e) \tag{2}$$

$$u\frac{\partial T}{\partial x} + v\frac{\partial T}{\partial y} = \frac{1}{(\rho C_p)_{hnf}}\frac{\partial}{\partial y}\left[k(T)\frac{\partial T}{\partial y}\right] + \tau\left(D_B\frac{\partial T}{\partial y}\frac{\partial C}{\partial y} + \frac{D_T}{T_\infty}\left(\frac{\partial T}{\partial y}\right)^2\right) - \frac{1}{(\rho C_p)_{hnf}}\frac{\partial q_r}{\partial y} +$$

$$\beta k_r^2 (C - C_\infty)\left(\frac{T}{T_\infty}\right)^n e^{\left(\frac{-E_a}{k_0 T}\right)} \quad (3)$$

$$u\frac{\partial C}{\partial x} + v\frac{\partial C}{\partial y} = D_B\frac{\partial^2 C}{\partial y^2} + \frac{D_T}{T_\infty}\frac{\partial^2 T}{\partial y^2} - k_r^2 (C - C_\infty)\left(\frac{T}{T_\infty}\right)^n e^{\left(\frac{-E_a}{k_0 T}\right)} \quad (4)$$

**Subject to the following boundary conditions**

$$u = u_w = \delta U_o x, v = 0, \ T = T_w, \ C = C_w \ , \quad at\ y = 0$$

$$u \to u_e = U_0 x, T \to T_\infty, C \to C_\infty, \quad as\ y \to \infty \quad (5)$$

where the component of velocity for $x$ and $y$ axes are $u$ and $v$ respectively, $u_e$ stands for the free stream velocity, $\delta$ is the parameter for plate velocity, $B$ represents the magnetic parameter, $\beta$ is the exothermic parameter,$\mu$ is the fluid viscosity, $k$ stands for thermal conductivity, $\beta_c$ is the casson parameter, $q_r$ stands for radiative heat flux, $k_r$ is the chemical reaction rate constant, $T_\infty$ represents the free stream temperature, $T_w$ is the wall temperature, $D_B$,stands for the diffusion coefficient, $\tau$ is the fluid heat capacity ratio, $C_\infty$ is the ambient fluid concentration while $C_w$ is the concentration at the wall, $\left(\frac{T}{T_\infty}\right)^n e^{\left(\frac{-E_a}{k_0 T}\right)}$ denotes the Arrhenius function. In addition, the density of hybrid nanofluid $\rho_{hnf}$, viscosity of hybrid nanofluid $\mu_{hnf}$, heat capacity of hybrid nanofluid $\left(\rho C_p\right)_{hnf}$, thermal conductivity of hybrid nanofluid $K_{hnf}$ are as follows [16,17]:

$$\rho_{hnf} = (1-\omega_2)\left[(1-\omega_1)\rho_f + \omega_1\rho_{s1}\right] + \omega_2\rho_{s2}, \qquad \mu_{hnf} = \frac{\mu_f}{(1-\omega_1)^{2.5}(1-\omega_2)^{2.5}},$$

$$\left(\rho C_p\right)_{hnf} = (1-\omega_2)\left[(1-\omega_1)\left(\rho C_p\right)_f + \omega_1\left(\rho C_p\right)_{s1}\right] + \omega_2\left(\rho C_p\right)_{s2},$$

$$K_{hnf} = \frac{k_{s2} + 2k_{nf} - 2\omega_2(k_{nf} - k_{s2})}{k_{s2} + 2k_{nf} + \omega_2(k_{nf} - k_{s2})} \times \frac{k_{s1} + 2k_f - 2\omega_1(k_f - k_{s1})}{k_{s1} + 2k_f + \omega_1(k_f - k_{s1})} \times k_f, \quad (6)$$

where $\rho_{s1}, \omega_1, \left(\rho C_p\right)_{s1}, k_{s1}$ are the thermophysical properties for gold nanoparticle, $\rho_{s2}, \omega_2, \left(\rho C_p\right)_{s2}, k_{s2}$ are the thermophysical properties for silver nanoparticle, $\rho_f, \mu_f, \left(\rho C_p\right)_f, k_f$ are the thermophysical properties for the base fluid.

**Table 1.** Thermophysical Properties of some nanofluids [17, 18]

| **Material** | **Density $(kg/m^3)$** | **Specific Heat Capacity $C_p(J/KgK)$** | **Thermal Conductivity $K(W/mk)$** |
|---|---|---|---|
| Sodium Alginate | 989 | 4175 | 0.6376 |
| Gold (Au) | 19300 | 129 | 318 |
| Silver $(Ag)$ | 10500 | 235 | 429 |

The Roseland approximation for radiation [19]:

$$q_r = -\frac{4\sigma^*}{3k^*}\frac{\partial T^4}{\partial y}, \quad (7)$$

Using Taylor's series and neglecting higher order terms for the expansion of $T^4$ about $T_\infty$, we finally have the radiation term in equation (3) to be

$$\frac{\partial q_r}{\partial y} = \left(-\frac{16\sigma^* T_\infty^3}{3k_1}\frac{\partial^2 T}{\partial y^2}\right) \tag{8}$$

Introducing the established similarity variables and stream function $\psi$ as used by Animasaun [20], Prasad *et al.*[21] as

$$\theta(\eta) = \frac{T - T_\infty}{T_w - T_\infty}, \qquad \phi(\eta) = \frac{C - C_\infty}{C_w - C_\infty}, \psi = \sqrt{\vartheta U_0}\, x f(\eta), \ \ \eta = y\sqrt{\frac{U_0}{\vartheta}}, \qquad u = \frac{\partial \psi}{\partial y}, v = \frac{\partial \psi}{\partial x} \tag{9}$$

For this study, the fluid viscosity and thermal conductivity are taken to be linear function of temperature [20 – 22] in the form

$$\mu(T) = \mu^*[1 + b(T_w - T)]\,, k = K[1 + \gamma(T - T_\infty)] \tag{10}$$

## 3 Method of Solution

Using equations (1) – (5), and variables (6) – (10), the continuity equation (1) is automatically satisfied and the governing equations reduced to the following ordinary differential equations:

$$\frac{df}{d\eta}\frac{df}{d\eta} - f(\eta)\frac{d^2 f}{d\eta^2} + \frac{\boldsymbol{\xi}\left(1 + \frac{1}{\beta_c}\right)}{(1-\omega_1)^{2.5}(1-\omega_2)^{2.5}\left\{(1-\omega_2)\left[(1-\omega_1) + \frac{\omega_1 \rho_{s_1}}{\rho_f}\right] + \frac{\omega_2 \rho_{s_2}}{\rho_f}\right\}}\frac{d^2 f}{d\eta^2}\frac{\boldsymbol{d\theta}}{\boldsymbol{dy}}$$

$$- \frac{(\boldsymbol{a} + (\boldsymbol{1} - \theta)\xi)\left(1 + \frac{1}{\beta_c}\right)}{(1-\omega_1)^{2.5}(1-\omega_2)^{2.5}\left\{(1-\omega_2)\left[(1-\omega_1) + \frac{\omega_1 \rho_{s_1}}{\rho_f}\right] + \frac{\omega_2 \rho_{s_2}}{\rho_f}\right\}}\frac{d^3 f}{d\eta^3} - 1$$

$$+ \frac{H_a}{\left\{(1-\omega_2)\left[(1-\omega_1) + \frac{\omega_1 \rho_{s_1}}{\rho_f}\right] + \frac{\omega_2 \rho_{s_2}}{\rho_f}\right\}}\left(\frac{df}{d\eta} - 1\right) = 0 \tag{11}$$

$$P_r f(\eta)\frac{d\theta}{d\eta} + \frac{\theta\epsilon}{\left[(1-\omega_2)\left[(1-\omega_1) + \frac{\omega_1 (\rho C_p)_{s_1}}{(\rho C_p)_f}\right] + \frac{\omega_2 (\rho C_p)_{s_2}}{(\rho C_p)_f}\right]}\frac{d\theta}{d\eta}\frac{d\theta}{d\eta} +$$

$$\frac{(1 + \theta\epsilon)}{\left[(1-\omega_2)\left[(1-\omega_1) + \frac{\omega_1 (\rho C_p)_{s_1}}{(\rho C_p)_f}\right] + \frac{\omega_2 (\rho C_p)_{s_2}}{(\rho C_p)_f}\right]}\frac{d^2\theta}{d\eta^2} + P_r N_b \frac{d\theta}{d\eta}\frac{d\phi}{d\eta} + P_r N_t \frac{d\theta}{d\eta}\frac{d\theta}{d\eta} +$$

$$\frac{P_r \beta^* C_r (1 + T_d\theta)^n e^{\left(\frac{-E_1}{(1+T_d\theta)}\right)}\phi}{T_d} + \frac{4}{3R_a\left[(1-\omega_2)\left[(1-\omega_1) + \frac{\omega_1 (\rho C_p)_{s_1}}{(\rho C_p)_f}\right] + \frac{\omega_2 (\rho C_p)_{s_2}}{(\rho C_p)_f}\right]}\frac{d^2\theta}{d\eta^2} = 0 \tag{12}$$

$$\frac{d^2\phi}{d\eta^2} + L_e f\frac{d\phi}{d\eta} + \frac{N_t}{N_b}\frac{d^2\theta}{d\eta^2} - L_e C_r \phi(1 + T_d\theta)^n e^{\left(\frac{-E_1}{(1+T_d\theta)}\right)} = 0 \tag{13}$$

**Subject to the boundary conditions**

$$\frac{df(0)}{d\eta} = \delta, \qquad f(0) = 0, \qquad \theta(0) = 1, \qquad \phi(0) = 1,$$

$$\frac{df(\infty)}{d\eta} \to 1 \qquad \theta(\infty) \to 0, \qquad \phi(\infty) \to 0 \tag{14}$$

Here, Chemical reaction rate parameter $C_r = \frac{k_r^2}{U_0}$ , activation energy parameter $E_1 = \frac{E_a}{k_0 T_\infty}$, Local magnetic parameter $H_a = \frac{\sigma B^2}{\rho_f U_0}$ , Temperature dependent thermal conductivity parameter $\epsilon = \gamma(T_w - T_\infty)$, Temperature dependent viscosity parameter $\xi = b(T_w - T_\infty)$, Lewis number $L_e = \frac{\vartheta}{D_B}$ , Brownian motion parameter $N_b = \frac{\tau D_B}{\vartheta T_\infty}(C_w - C_\infty)$ , thermophoretic parameter $N_t = \frac{\tau D_T}{\vartheta T_\infty}(T_w - T_\infty)$, Prandtl number $P_r = \frac{(\rho c_p)_f \vartheta}{K_f}$ , Radiation parameter $R_a = \frac{k_f k_1}{4\sigma^* T_\infty^3}$ , temperature difference parameter $T_d = \frac{(T_w - T_\infty)}{T_\infty}$, exothermic/endothermic parameter $\beta^* = \beta(C_w - C_\infty)$.

The physical qualities of engineering interest in this study are the skin friction coefficient$c_f$, local Nusselt number $Nu_f$and Sherwood number $S_h$ which are defined as

$$C_f = \frac{\tau_w}{\rho_f U^2} \ , Nu_x = \frac{x q_w}{k_f (T_w - T_\infty)}, Sh = \frac{x J_w}{D(C_w - C_\infty)} , \tag{15}$$

and

$$\tau_w = \mu_{hnf} \left(\frac{\partial u}{\partial y}\right)_{y=0} , \quad q_w = -k_{hnf} \left(\frac{\partial T}{\partial y}\right)_{y=0} + (q_r)_{y=0} , \quad J_w = -D_B \left(\frac{\partial C}{\partial y}\right)_{y=0} \tag{16}$$

### 3. Numerical Solution

The coupled ordinary differential equations (11) – (13) and their corresponding boundary conditions (14) are first reduced to a system of first order equations using the method of superimposition [23]. The following variables are often being employed in the method of superimposition:

$$f = f_1, \ f' = f_2, \ f'' = f_3, \theta = f_4, \ \theta' = f_5, \ \phi = f_6, \ \phi' = f_7. \tag{17}$$

Based on (17) above, equations (11) – (13) reduce to

$$f_3' = \frac{A_1 A_2}{(\boldsymbol{a} + (\mathbf{1} - \theta)\xi)\left(1 + \frac{1}{\beta_c}\right)} \left\{ f_2 f_2 - f_1 f_3 + \frac{\boldsymbol{\xi}\left(1 + \frac{1}{\beta_c}\right)}{A_1 A_2} f_3 f_5 - 1 + \frac{H_a}{A_2}(f_2 - 1) \right\} \tag{18}$$

$$f_5' = \frac{3R_a A_3}{4 + 3R_a(1 + f_4 \epsilon)} \left\{ \begin{array}{c} -P_r f_1 f_5 - \frac{f_4 \epsilon}{A_3} f_5 f_5 - P_r N_b f_5 f_7 - P_r N_t f_5 f_5 \\ -\frac{P_r \beta^* C_r (1 + T_d f_4)^n e^{\left(\frac{-E_1}{(1+T_d f_4)}\right)} f_6}{T_d} \end{array} \right\} \tag{19}$$

$$\frac{d^2\phi}{d\eta^2} = -L_e f_1 f_7 - \frac{N_t}{N_b} f_5' + L_e C_r f_6 (1 + T_d f_4)^n e^{\left(\frac{-E_1}{(1+T_d f_4)}\right)} \tag{20}$$

subject to

$$f_2(0) = \delta, \ f_1(0) = 0, \ f_4(0) = 1, \ f_6(0) = 1, \quad f_2(\infty) \to 1, f_4(\infty) \to 0, f_6(\infty) \to 0 \tag{21}$$

where $A_1 = (1 - \omega_1)^{2.5}(1 - \omega_2)^{2.5}, A_2 = \left\{(1 - \omega_2)\left[(1 - \omega_1) + \frac{\omega_1 \rho_{s_1}}{\rho_f}\right] + \frac{\omega_2 \rho_{s_2}}{\rho_f}\right\}$,

$$A_3 = \left[(1-\omega_2)\left[(1-\omega_1) + \frac{\omega_1(\rho C_p)_{s_1}}{(\rho C_p)_f}\right] + \frac{\omega_2(\rho C_p)_{s_2}}{(\rho C_p)_f}\right].$$

This system of equations (18) – (21) are thereafter solved numerically using the Matlab bvp5c solver.

## 4. Results and Discussion

In order to analyze the results, numerical computation has been carried out for various values of Hartmann number$(H_a)$, fluid material parameter $(\beta_c)$, Lewis number $(L_e)$, Prandtl number $(P_r)$, thermal conductivity parameter $(\epsilon)$, thermophoretic parameter $(N_t)$ and velocity parameter $(\delta)$, using the numerical scheme discussed in the previous section. The numerical values obtained from the result are plotted in Figures 2 –12.

The influence of velocity ratio parameter on fluid velocity was graphically illustrated in Figure 2. It was observed that at both $\delta < 1$ and $\delta > 1$, fluid velocity increases with velocity ratio. At $\delta = 1$, which means stretching and free stream velocities are equal, no boundary layer is formed. Physical interpretation of $\delta < 1$ is that stretching velocity exceeds free stream velocity while $\delta > 1$ means the free stream velocity surpasses the stretching velocity. The variation in velocity with respect to Casson fluid parameter $(\beta_c)$ was graphically illustrated in Figure 3. The figure also showed that the hybrid nanofluid performed better in increasing the velocity than the conventional nanofluid and conventional fluid. The figure showed that velocity profile increases with Casson fluid parameter. An increase in Casson fluid parameter implies a decrease in yield stress and a resultant increase in plastic viscosity which leads to decrease in velocity but the decrease in velocity which is expected is overpowered by high temperature due to the kind of reaction in the system. This observation is similar to Figure 2 reported by Animasaun [20].

The effect of radiation parameter on the fluid temperature is illustrated in Figure 4. The figure revealed that temperature reduces for increase in radiation parameter. The reason for this decrease in temperature is because large values of radiation parameter correspond to an increase in dominance of conduction over radiation, thus decreasing the thickness of the thermal boundary layer and increasing the heat loss to the ambient. Similar decrease in temperature due to increase in radiation parameter was reported in Figure 7 by Abdul Maleque [12], Figure 12 of Koriko *et al* [24] and Figure 13 by Zaib *et al.*[19]. Figure 5 illuminates the variation in concentration caused by a change in thermophoretic parameter. The figure demonstrated that the concentration field is an increasing function of thermophoretic

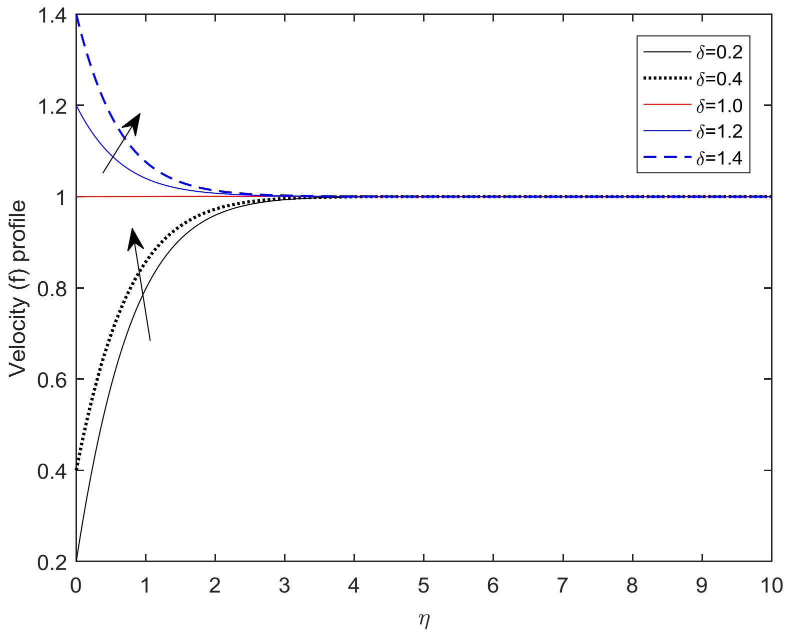

Figure 2: Variation in velocity ratio parameter with Velocity

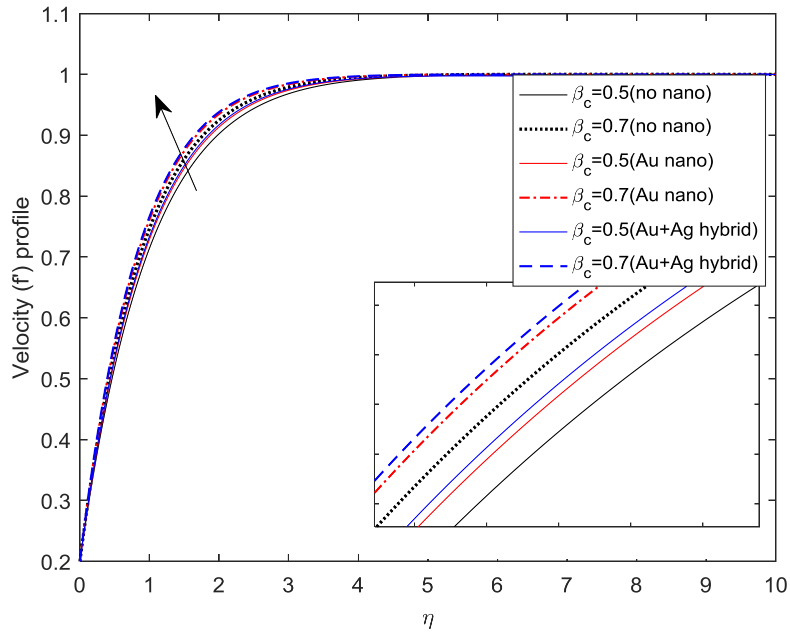


Figure 3: Variation in Casson parameter $(\beta_c)$ with Velocity

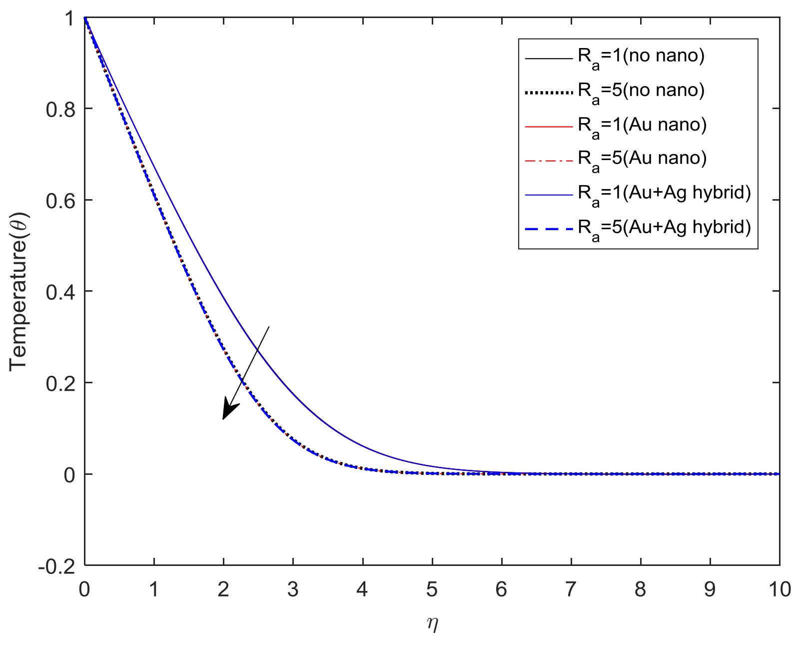


Figure 4: Variation in Radiation parameter with Temperature

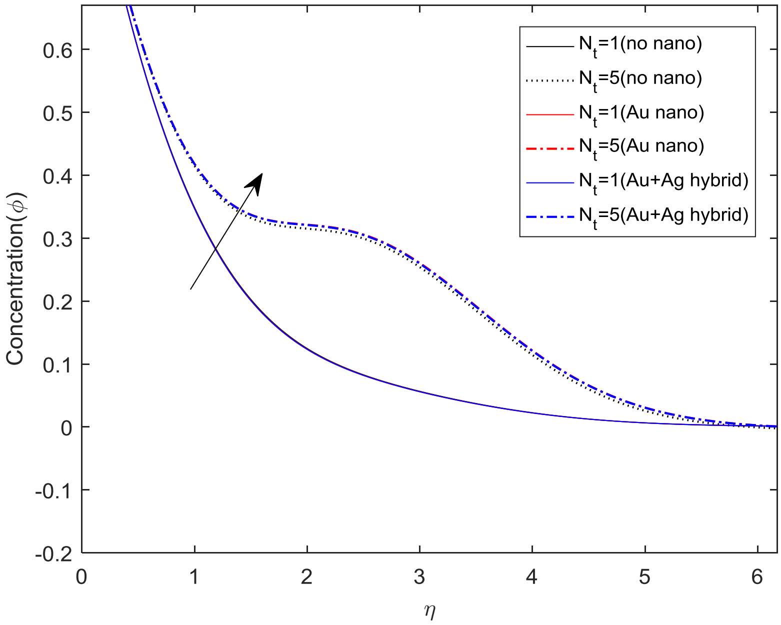


Figure 5: Variation in thermophoretic parameter$(N_t)$ with Concentration

parameter. This observation is in good harmony with Fig. 14 reported in Shehzad *et al*. [22]. Variation in thermal conductivity with velocity is being exhibited in Figure 6. The figure revealed that the fluid flow increases with thermal conductivity. The reason for this behavior is that thermal conductivity$(\epsilon)$ is linearly proportional to temperature. So, as the $\epsilon$ causes temperature to rise, the fluid viscosity reduces, hence fluid motion increases.

Figure 7 illuminates the impact of chemical reaction on temperature. The figure exhibited that chemical reaction reduces fluid temperature. This observation is in harmony with Figure 5 reported by Abdul Maleque [12]. The influence of chemical reaction parameter on fluid concentration is graphically represented in Figure 8. The figure revealed that chemical reaction parameter suppresses fluid concentration. The physical significance of this, is that the number of solute molecules undergoing chemical reaction increases as chemical reaction parameter increases although other parameters(conditions) are constant, this therefore results in decrease in the concentration profile. This is in good agreement with Figure 15 reported by Kiran Kumar *et al.* [25], Fig. 3 reported by Kalaivanan *et al.*[26] and Figure 12 reported by Mahanthesh *et al.* [27]. The influence of activation energy parameter $(E_1)$ on velocity is elucidated in Figure 9. The figure showed that activation energy increases fluid flow. Figure 10 revealed the impact of activation energy on fluid concentration. The figure elucidated that activation energy enhances the concentration profile. This is because an higher energy activation and weaker temperature leads to lower rate of reaction, which results in lesser chemical reaction and thus fluid concentration increases. This is in good agreement with Figure 13 in Kiran Kumar *et al.*[25] and Fig. 7 reported by Azam *et al.* [28].

The influence of exothermic reaction parameter $(\beta)$ on fluid velocity was graphically represented in figure 11. The figure showed that exothermic reaction aids fluid flow. A similar effect was shown in Figure 12 on temperature fueled by the exothermic reaction.

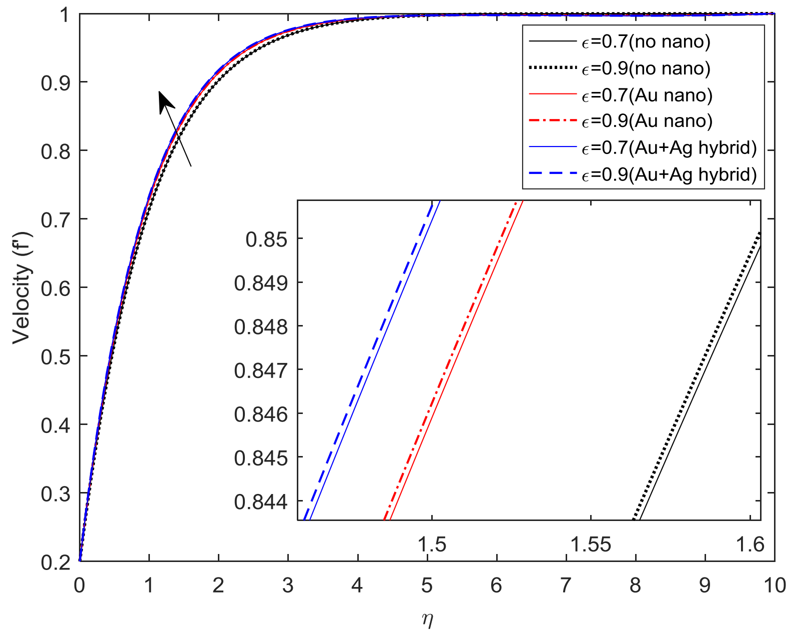


Figure 6: Variation in thermal conductivity parameter $(\epsilon)$ with velocity

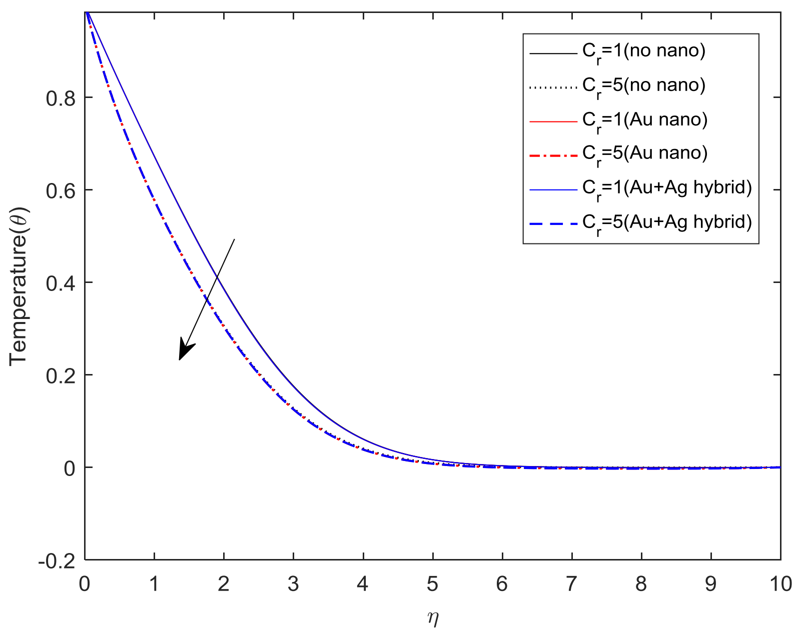


Figure 7: Variation in Chemical reaction parameter $(C_r)$ with Temperature

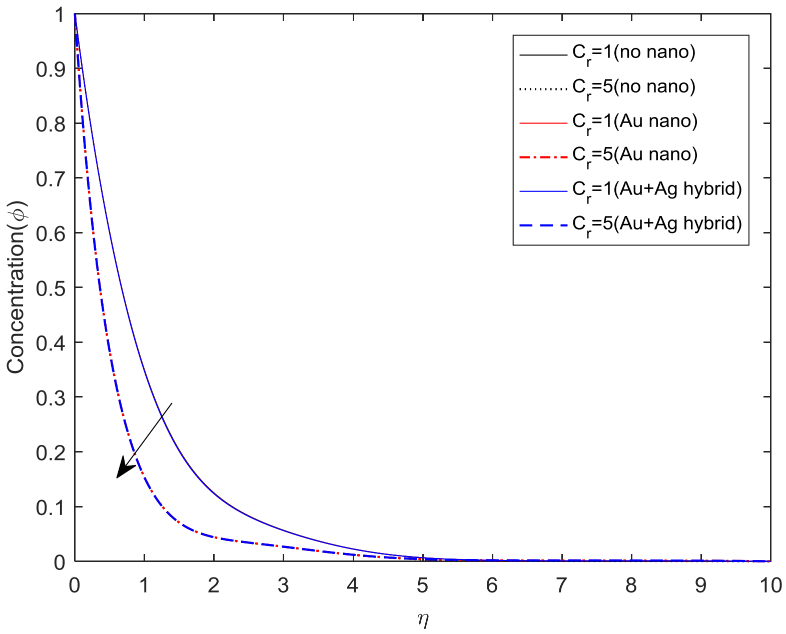


Figure 8: Variation in Chemical reaction parameter $(C_r)$ with concentration

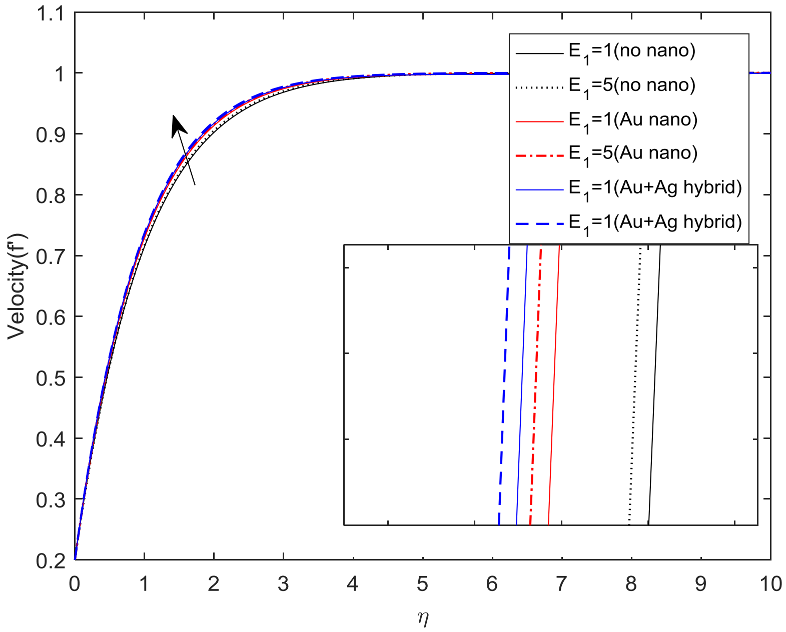


Figure 9: Variation in Activation energy parameter $(E_1)$ with Velocity

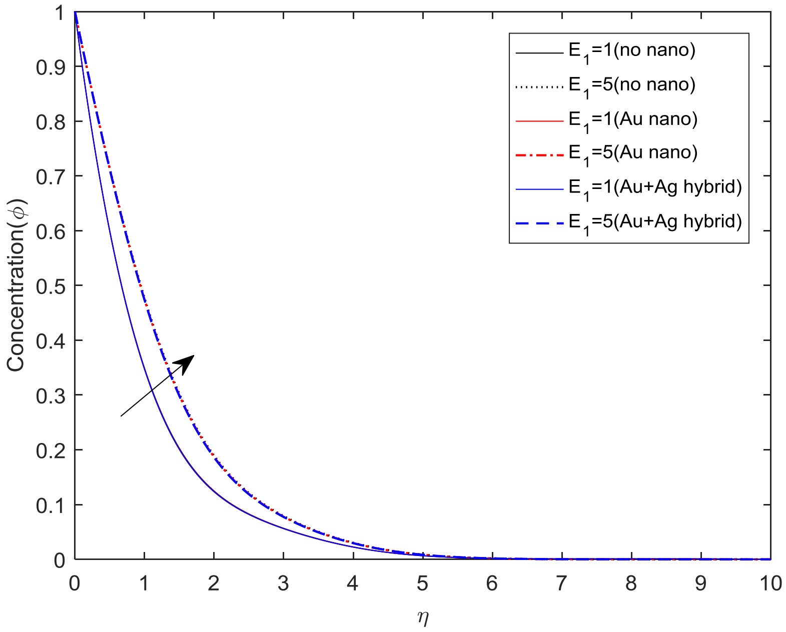


Figure 10: Variation in Activation parameter $(E_1)$ with Concentration

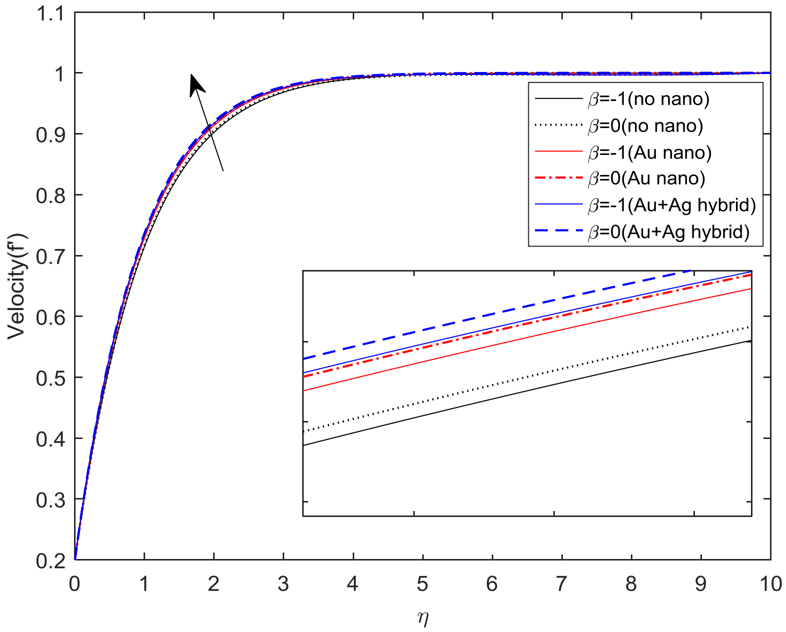


Figure 11: Variation in Exothermic parameter $(\beta)$ with Velocity

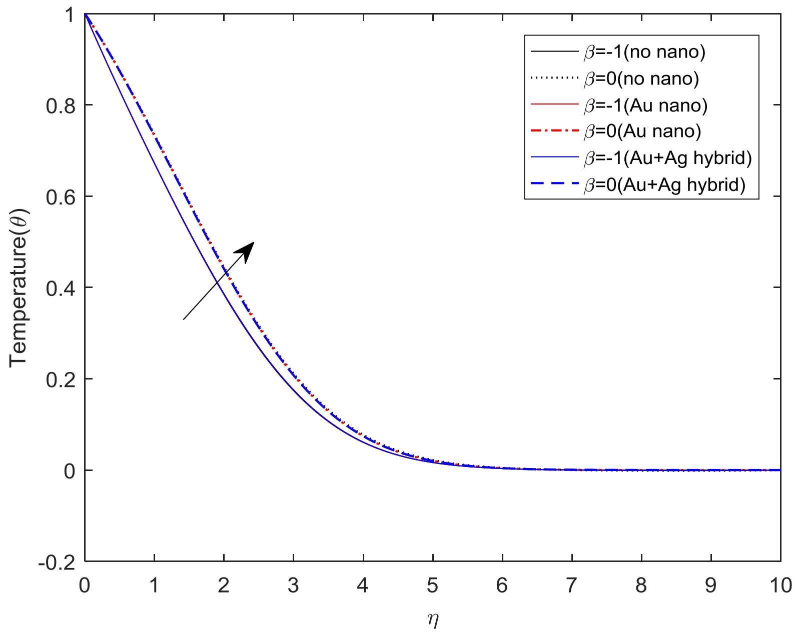


Figure 12: Variation in Exothermic parameter $(\beta)$ with Temperature

## 5. Conclusion

The analysis on the exothermic chemical reaction on the forced convection flow of a thermally radiative non-Newtonian based hybrid nanofluid have been conducted and the following obtained:

(1) Fluid flow increases by increasing any of velocity ratio, thermal conductivity, activation energy, Casson fluid, exothermic reaction parameters.
(2) Chemical reaction and radiation parameters force a reduction in fluid velocity for an exothermic reaction of a non-Newtonian hybrid nanofluid.
(3) Thermophoresis increases fluid concentration but chemical reaction reduces fluid concentration.
(4) Hybrid nanofluid showed better performance over conventional nanofluid and convectional fluid in test involving fluid parameter, thermal conductivity, activation energy, exothermic reaction and velocity.

## References


[1] Moshizi S. A. Forced convection heat and mass transfer of MHD nanofluid flow inside a porous microchannel with chemical reaction on the walls. *Engineering Computations* (2015), Vol. 32,8, pp. 2419 – 2442.

[2] Trombetta M.L. Laminar Forced Convection in Eccentric Annuli. *International Journal of Heat and Mass Transfer*, Vol. 14, pp. 1161 – 1173 - Pegamon Press 1971, Great Britain.

[3] Beckermann C. and Viskanta R. Forced Convection Boundary Layer Flow and Heat Transfer along a Flat Plate embedded in a Porous Medium. *International Journal of Mass Transfer*, 1987,Vol. 30, No.7,pp. 1547 – 1551.

[4] Childs PRN, Long C. A Review of Forced Convective Heat Transfer in Stationary and Rotating Annuli – *Proceedings of the Institution of Mechanical Engineers, Part C: Journal of Mechanical Engineering Science,* 1996, ISSN: 0954 – 4062.

[5] Salleh M.Z., Nazar R. and POP I. Forced Convection Boundary Layer Flow at a Forward Stagnation Point with Newtonian Heating, *Chemical Engineering Communications*, 2008, 196:9, 987 – 996, DOI: 0.1080/00986440902797840

[6] Choi S.U.S. Enhancing thermal conductivity of fluids with nanoparticles. *ASME-Publicat Fe* (1995), 231: 99 – 106.

[7] Suresh S., Venkitaraj K.P., Selvakumar P. and Chandrasekar M. Effect of Al2O3–Cu/water hybrid nanofluid in heat transfer, *Experimental Thermal and Fluid Science* 38, 54–60 (2012).

[8] Nadeem S, ABBAS N and Khan A.U. Characteristics of three dimensional stagnation point flow of Hybrid nanofluid past a circular cylinder, *Results in physics* 8(2018), 829–835.

[9] Gul T, Bilal M., Khan A., Aedh Alreshidi N, Mukhtar S, Shah Z. and Kumam P. Magnetic Dipole impact on Hybrid nanofluid Flow over an Extending Surface, *Scientific Reports (Nature Publisher Group)*, 10(2020), Iss.1. doi.org/10.1038/s41598-020-65298-1.

[10] Aladdin N.A.L., Bachok N and Pop I. Cu-$Al_2O_3$/water hybrid nanofluid flow over a permeable moving surface in presence of hydromagnetic and suction effects. *Alexandria Engineering Journal* (2020), 59, 657 – 666.

[11] Rashidi M.M, Sadri M., Sheremet M.A. Numerical Simulation of Hybrid Nanofluid Mixed Convection in a Lid-Driven Square Cavity with Magnetic Field Using High-Order Compact Scheme - *Nanomaterials* (2021), 11, 2250. https://doi.org/10.3390/nano11092250

[12] Abdul Maleque Kh. Effects of Exothermic/Endothermic Chemical Reactions with

[13] Arrhenius Activation Energy on MHD Free Convection and Mass Transfer Flow in Presence of Thermal Radiation. *Journal of Thermodynamics*, Volume 2013, Article ID 692516, 11 pages, http://dx.doi.org/10.1155/2013/692516.

[14] Sharma B.K., Gandhi R., Al-Mdallal Q.M. Entropy generation minimization of higher order endothermic/exothermic chemical reaction with activation energy on MHD mixed convective flow over a stretching surface. Sci Rep 12, 17688(2022).

[15] Abdel-Galed S.M and Hamad M.A.A. MHD Forced Convection Laminar Boundary Layer Flow of Alumina-Water Nanofluid over a Moving Permeable Flat plate with Convective Surface Boundary Condition, *Journal of Applied Mathematics*, Volume 2013, Article ID 403210, http://dx.doi.org/10.1155/2013/403210.

[16] Salawu S.O., Fatunmbi E.O., Okoya S.S. MHD heat and mass transport of Maxwell Arrhenius kinetic nanofluid flow over stretching surface with nonlinear variable properties, *Results in Chemistry 3* (2021) 100125

[17] Hayat T, Nadeem S.(2017). Heat transfer enhancement with Ag–CuO/ water hybrid nanofluid, *Results Phys* 7(2017) : 2317–2324.

[18] Jawad M, Saeed A, Tassaddiq A, Khan A, Gul T., Kuman P., Shah Z.(2021). Insight into the dynamics of Second Grade Hybrid Radiative Nanofluid Flow with the Boundary Layer Subject to Lorentz Force, *Scientific Reports* (2021), 11, 4894, Doi.org/10.1038/s41598-021-84144-6.

[19] Mekheimer K.S., Hasona W.M, Abo-Elkhair R.E, Zaher A.Z. Peristaltic Blood Flow with Gold Nanoparticles as a Third Grade Nanofluid in Catheter: Application of Cancer Therapy, *Physics Letters A* 382 (2018): 85–93

[20] Zaib A., Chamkha A.J, Rashidi M.M. and Bhattacharyya K Impact of nanoparticles on flow of a special non-Newtonian third-grade fluid over a porous heated shrinking sheet with nonlinear radiation, *Nonlinear Engineering* (2018) 7(2): 103– 111.

[21] Animasaun I.L. Effects of thermophoresis, variable viscosity and thermal conductivity on free convective heat and mass transfer of anon-darcian MHD dissipative Casson fluid flow with $n^{th}$ order chemical reaction. *Journal of Mathematical Society* 34(2015):11 – 31.

[22] Prasad K.V, Vajravelu K, Datti P.S. The effects of variable fluid properties on the hydromagnetic flow and heat transfer over a non-linearly stretching sheet, *Int. J. Ther. Sci.*, 49(2010) 603‑10.

[23] Shehzad S.A, Tariq Hussain, Hayat T, Ramzan M., Alsaedi A. Boundary layer flow of third grade nanofluid with Newtonian heating and viscous dissipation, *Journal of Central South University* 22(2015), 360 – 367.

[24] NA T.Y. Computational Methods in Engineering Boundary Value Problems, *New York (1979): Academic Press*.

[25] Koriko I.K, Omowaye A.J., Animasahun I.L., Babatunde I.O. Boundary Layer Analysis of Exothermic and Endothermic Kind of Chemical Reaction in the Flow of Non-Darcian Unsteady Micropolar Fluid along an Infinite Vertical Surface. *International Journal of Engineering Research in Africa*, Vol. 28, pp 90-101, doi:10.4028/www.scientific.net/JERA.28.90

[26] Kiran Kumar R.V.M.S.S., Vinod Kumar G., Raju C.S.K., Shehzad S.A., Varma S.V.K. Analysis of Arrhenius Energy in Magnetohydrodynamic Carreau fluid flow through Improved theory of Heat diffusion and Binary Chemical Reaction. Journal of Physics Communications 2018, vol.2, 035004.

[27] Kalaivanan R., Vishnu Ganesh N., Qasem M. Al-Mdallal. An investigation on Arrhenius activation energy of second grade nanofluid flow with active and passive control of nanomaterials. *Case Studies in Thermal Engineering* 22 (2020) 100774.

[28] Mahanthesh B., Gireesha B.J., Rama Subba Reddy Gorla. Heat and mass transfer effects on the mixed convective flow of chemically reacting nanofluid past a moving/ stationary vertical plate, *Alexandria Eng. J.* (2016), http://dx.doi.org/10.1016/j.aej.2016.01.022

[29] Azam M., Xu T., Shakoor A., Khan M. Effects of Arrhenius activation energy in development of covalent bonding in axisymmetric flow of Radiative-Cross nanofluid, *International Communications in Heat and Mass Transfer* 113 (2020) 104547.